Determination of energy thresholds of electron excitations at semiconductor/insulator interfaces using trap-related displacement currents

V.V. Afanas'ev[1], J. Schubert[2], A. Neft[2,3], G. Delie[1], I. Shlyakhov[1], V. Trepalin[1], M. Houssa[1], A. Stesmans[1]

[1]*Semiconductor Physics Laboratory, University of Leuven, 3001 Leuven, Belgium*

[2]*PGI 9-IT, Forschungszentrum Jülich GmbH, 52425 Jülich, Germany*

[3]*Saint-Gobain Sekurit Deutschland GmbH & CO. KG, 52134 Herzogenrath, Germany*

e-mail address of corresponding author: valeri.afanasiev@fys.kuleuven.be

Abstract Spectral measurements of illumination-induced displacement currents related to trapping of charge carriers optically excited in semiconductor electrodes are shown to deliver information regarding energy onsets of electron transitions at the interface. Presented examples include determination of the conduction band offset at the GaN/Al_2O_3 interface and determination of charge carrier excitation spectra of two-dimensional (2D) semiconductors MoS_2 and WS_2 at the interface with insulating SiO_2.

1. Introduction

Re-distribution of charges in metal-insulator-semiconductor (MIS) or metal/insulator/metal (MIM) structures is well known to induce transient displacement currents in an external electrical circuit [1]. One may also expect that electron transitions to and from traps in the insulating film will give rise to similar currents reflecting variations in the net trapped charge due to changes in trap occupancy. Would illumination of the sample affect the electron trapping rate by generating additional carriers at energies allowing transition to the traps, the corresponding energy thresholds will be reflected in the spectral dependences of the generated in this way displacement current [2]. Since the trapping of the optically excited charge carriers may occur directly from the electrode material by tunneling or upon injection into the insulator band two types of spectral thresholds can be detected: The onset of the charge carrier generation in semiconductor electrode corresponding to the bandgap width and the onset of electron photoemission from the electrode into the near-interface insulating layer. These transitions are schematically shown in Fig. 1(a) as photoconductivity (PC) and internal photoemission (IPE) processes, respectively. Obviously, both PC and IPE can also be observed using more conventional dc current measurements using the same measurement arrangement illustrated in Fig. 1(b) [3,4]. However, the dc photocurrent measurements are often impaired by leakage current or by high layer resistance as it happen in the case of few-monolayer (ML) thin films. In this work we will show that spectrally-resolved measurements of trap-related displacement current allows one to improve significantly on characterization of electron states at semiconductor/insulator interfaces. Examples presented here pertain to interfaces of three-dimensional (3D) semiconducting GaN as well as two-dimensional (2D) single-ML MoS_2 and WS_2 semiconductor films with two widely used oxide insulators, i.e., SiO_2 and Al_2O_3.

2. Experimental

The GaN/Al_2O_3 samples were prepared on heavily doped n-type ($n \approx 1x10^{18} cm^{-3}$) 2 μm thick (0001) GaN epitaxial layer on sapphire substrate. After 3 min GaN surface clean in aqueous HCl solution (HCl:H_2O = 1:4) a 20-nm thick amorphous (a-) Al_2O_3 layer was grown by pulsed-laser oxide deposition (PLD) at 560 °C. Photoelectric measurements [Fig. 1(b)]

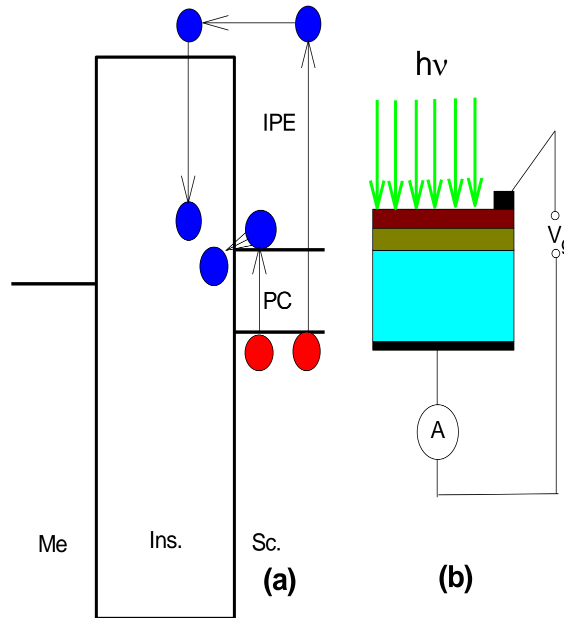

Figure 1. (a) Schematics of electron transitions from semiconductor electrode to traps in the near-interface insulating layer due to optical excitation of intrinsic photoconductivity (PC) and internal photoemission (IPE). (b) Experimental scheme of photocurrent measurements in MIS structure with semitransparent top electrode.

were performed on MIS capacitors fabricated by thermoresistive evaporation of semitransparent (15 nm thick) Au electrodes of 0.5 mm^2 area on top of the a-Al_2O_3 layer. Electrical contact to the bottom GaN layer was ensured by evaporation of 100-nm thick blanket Al contact layer on the sample periphery.

The Si/SiO_2/MoS_2 and Si/SiO_2/WS_2 structures were prepared on heavily doped p-type Si(100) (p≈10^{20}cm^{-3}) substrates with thermally grown 50-nm thick SiO_2 insulator. Single- and few-ML MoS_2 and WS_2 were grown on top of SiO_2 at 800 °C from $Mo(CO)_6$ and $W(CO)_6$ precursors, respectively, following the chemical vapor deposition (CVD) process described elsewhere [5]. Electrical contact to the disulfide semiconductor layers was done either by using non-transparent contact pads (Au or Al, 100 nm thick) [4,6] or by evaporation of semitransparent (15 nm) Au or Al electrodes of 0.5 mm^2 area. Back contact to Si substrate was fabricated by evaporation of 100-nm thick blanket Al layer.

Measurements were done at room temperature using the scheme shown in Fig. 1(b) when the capacitor structure biased by applying gate voltage (V_g) to the top electrode is illuminated by monochromatic light of known photon energy hν. The photocurrent detected in the external circuit by Keithley 6517 electrometer was normalized to the incident photon flux to calculate the quantum yield (Y). This photocurrent was defined as the difference between currents measured under illumination (I_{light}) and in darkness (I_{dark}). In both cases the current was readout 30s after light was turned on/off, with 50 averages per measurement at each hν.

3. Results

3.1 Electron injection at the GaN/a-Al_2O_3 interface

First we address determination of the conduction band (CB) offset at the n^+-GaN/a-Al_2O_3 interface. The photocurrent yield spectra measured on GaN/a-Al_2O_3/Au structure with positive and negative bias applied to the top semitransparent Au electrode are shown in Fig. 2 (a) and (b), respectively. For positive metal bias the current flow direction corresponds to electron injection from GaN and their drift towards the metal electrode. Though the energy onset of electron injection can be seen at hν≈ 2.2 eV, significant leakage current instability makes spectra noisy and limits the accuracy to ≈0.1-0.15 eV. Similar noisy spectra have earlier been reported for the Al_2O_3 layers grown on n-GaN using atomic layer deposition at 300 °C [7]. However, when the bias polarity is reversed, the dark leakage current is reduced dramatically due to negligible hole concentration in the used n^+-GaN and high energy barrier for electrons at the opposite Au/Al_2O_3 interface (≈4 eV [3]). For this bias polarity, the photocurrent yield spectra exhibit two distinct spectral regions: In the low energy range [$h\nu<E_g$(GaN)≈3.35 eV] the current flow direction corresponds to electron motion from GaN into the oxide, i.e., *against electric field*.

To get insight in the physical mechanism of this effect, we zoomed in the corresponding low-energy spectral range and analyzed the results as described in more detail in the Supplemental Material. Summarizing this analysis, the final state of the observed optical transitions corresponds to the lowest CB of a-Al_2O_3 at the interface with GaN while the initial state belongs to the energetically narrow distribution of electrons near the bottom edge of GaN CB. Therefore, the inferred spectral threshold of 2.20±0.05 eV corresponds to the CB offset at the GaN/a-Al_2O_3 interface. The latter can now be determined by far more accurately

than in the case of photoinjection current measured under positive bias with strong noise caused by I_{dark} instability (which is similar to that observed for ALD-grown a-Al_2O_3 in Ref.7).

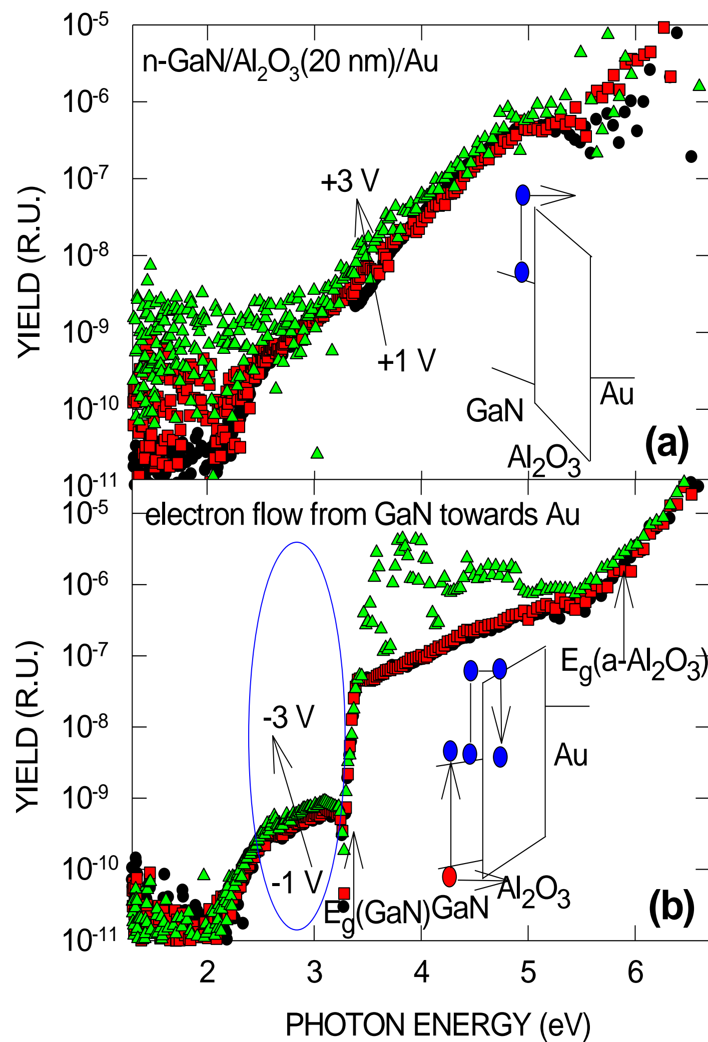

Figure 2. Semi-logarithmic plots of photocurrent yield spectra as measured on n^+-GaN/Al_2O_3/Au structures under positive (a) and negative (b) voltages applied to the semitransparent gold electrode. Insets illustrate the schemes of the observed electron transitions at the GaN/a-Al_2O_3 interface.

Next, when hν exceeds the GaN gap width, the photocurrent measured under negative bias abruptly increases by several orders of magnitude reversing to its "normal" polarity [cf. Fig. 2(b)] indicating injection of photogenerated holes from GaN into Al_2O_3. Besides allowing for direct GaN PC threshold determination (direct gap E_g= 3.36±0.05 eV), this result indicates a much reduced valence band (VB) offset at the GaN/a-Al_2O_3 interface: By combining the inferred CB offset and the GaN gap width with 6-eV wide gap of a-Al_2O_3 found from the oxide PC spectra [cf. vertical arrow in Fig. 2(b)], the VB offset of only ≈0.5 eV can be estimated. This explains easy injection of holes optically excited in GaN into a-Al_2O_3.

3.2 Electron excitations in few ML MoS_2 and WS_2 semiconductors on SiO_2

The second example concerns the use of displacement currents to measure the PC on single- or few-ML thin 2D semiconducting MoS_2 and WS_2. In the case of production-relevant large-area CVD synthetic films, direct PC measurements in co-planar geometry generally fail because of strong surface recombination. However, if performing photocurrent measurements in Si/SiO_2/MoS_2(WS_2) capacitors with metal contact layer or pad [6] evaporated on top of a few-ML semiconductor electrode it appears possible to detect not only the electron IPE from the semiconductor VB but, also, photocurrents in the low photon energy range. These currents correspond to generation of electron-hole pairs in the few-ML thick semiconductor. Fig. 3 compares the raw photocurrent spectra of 1ML MoS_2 and 1ML WS_2 directly grown by CVD on top of Si/SiO_2(50nm) substrates clearly demonstrating difference in the onset of PC and the additional structure (A- and B- excitonic transitions at lower and higher energies, respectively) consistent with optical absorbance spectra known from the literature. Therefore, variations in the optical absorption affecting the electron-hole pair generation rate appear to be directly reflected in the displacement current due to the corresponding change in the carrier trapping rate. Observation of excitonic peaks suggests that charge carrier trapping occurs from a bonded state, i.e., excitons dissociate as a result of trapping. Noteworthy, no photocurrents of this sort can be detected for the synthetic single- or few-ML graphene transferred onto the identical Si/SiO_2 substrates. The latter observation suggests that additional density of charge carriers generated in graphene during illumination is still insignificant compared to the electron density already present in the electrode in thermal equilibrium, i.e., in darkness.

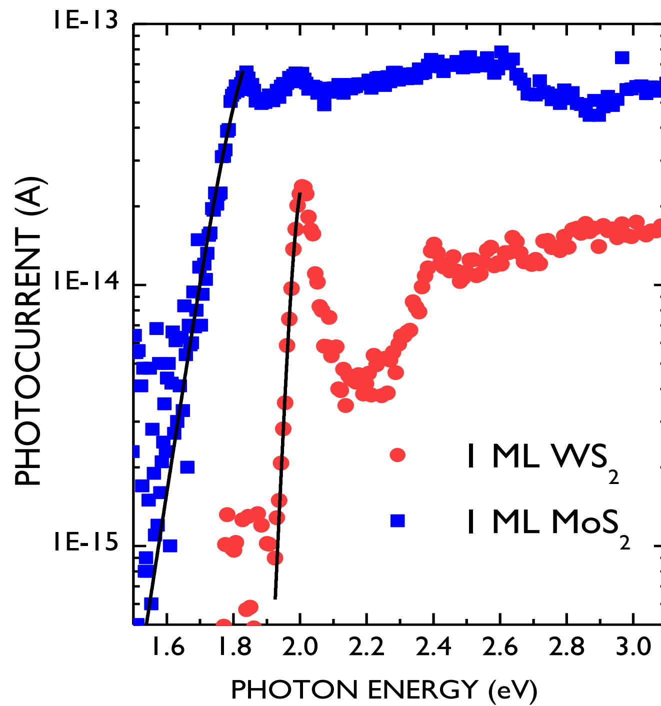

Figure 3. Semi-logarithmic photocurrent spectra as measured on Si/SiO_2 (50 nm) samples with single-ML MoS_2 (blue squares, V_g=-0.75 V) and WS_2 (red circles, V_g=-4 V) top electrodes contacted using a non-transparent Au contact pad.

Another interesting comparison concerns the photoresponse of unmetallized semiconductor film (contacted through a small non-transparent metal pad [4]) and the same film with a large area semitransparent (15-nm thick) metal contact evaporated directly on top of the 2-D material. The results are shown in Figs. 4 and 5 for few-ML (3.5 ML average thickness) MoS_2 and a single-ML WS_2, respectively. The spectra reveal considerable impact of Al evaporation on the PC of MoS_2 samples. The photocurrent onset at $h\nu\approx2.5$ eV suggests the optical excitation still occurring in the MoS_2 layer because the energy threshold of electron IPE from Al into SiO_2 is known to be significantly higher, in the range 3.1-3.3 eV [8].Apparently, there is a chemical interaction between the metal and MoS_2, possibly promoted by terrace edges found in this kind of samples characterized by the presence of 2-3 ML pyramid-like structures on top of 1-2 ML continuous MoS_2 underlayer (cf. surface morphology results shown in Fig. 3 in Ref.),

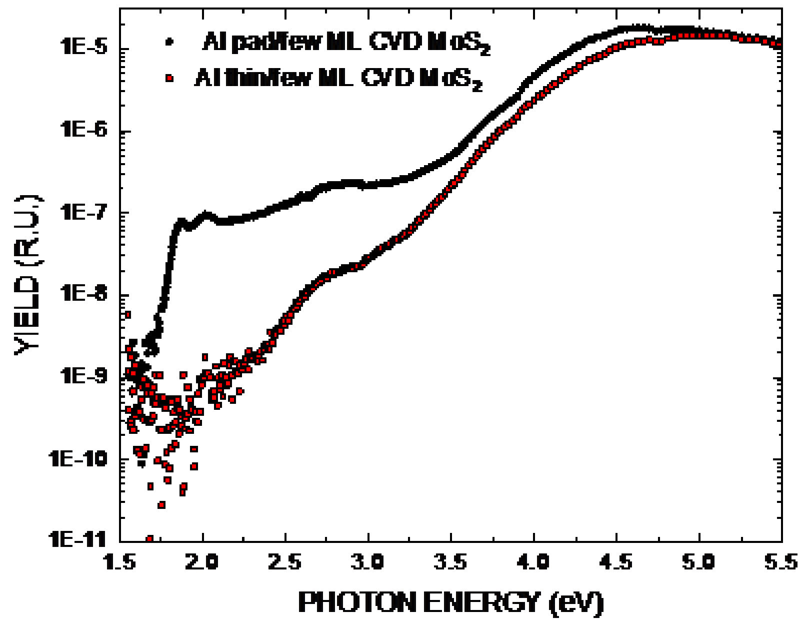

Figure 4. Semi-logarithmic plot of the photocurrent yield spectra measured on Si/SiO_2(50 nm) samples with few-ML MoS_2 (3.5 ML average coverage thickness) top electrodes contacted by using a small non-transparent Al pad (black rhombs) or a semitransparent (15 nm thick) Al electrode of 0.5 mm^2 area (red squares) under top electrode bias V_g=-3 V.

By contrast, the same semitransparent Al electrode evaporated on top of a single-ML WS_2 results in no spectrum change (cf. Fig. 5) except for the signal enhancement thanks to the larger area of the electrically contacted semiconductor. It appears then that a 1-ML of WS_2 is more chemically stable than the MoS_2 film with higher surface roughness. What probably is more important, is that the signal from semiconductor optical excitation is detectable beneath the contact metal overlayer which allows one to use the described here technique to analyze impact of the contact metals on the electron states in 2D semiconductors. Furthermore, because the semitransparent metal ensures reliable contact over its area, similar electrical characterization becomes possible even in the case of discontinuous 2D films comprising of isolated grains [9] which is often the case for newly-developed 2D materials. This unique possibility essentially depends on the presence of charge traps at the interface between 2D material and underlying insulating layer providing a rare example of the benign role of charge trapping might play in semiconductor research and technology.

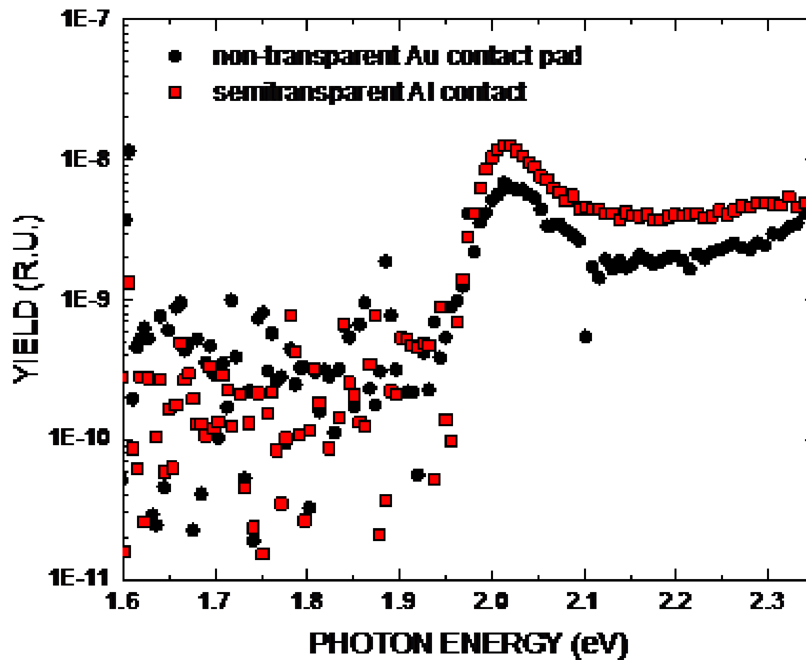

Figure 5. Semi-logarithmic plot of the photocurrent yield spectra measured on Si/SiO_2 (50 nm) samples with single-ML WS_2 top electrodes contacted by using a small non-transparent Au pad (black stars) or a semitransparent (15 nm thick) Al electrode of 0.5 mm^2 area (red squares). Top electrode bias during measurements is V_g=-10 V.

4. Conclusions

Observation of trapping-related displacement current spectral curves is demonstrated to deliver valuable information regarding energy onsets of electron excitations at interfaces of semiconductors with insulating films including bandgap width, optical resonance energies, and band offsets. In particular, this method appears to be useful to characterize interfaces of single- or few-ML 2D semiconductors which can hardly be assessed using the more conventional approaches to electrical measurements.

References

[1] P. DeVisschere, The validity of Ramo's theorem, Solid State Electron. 33 (1990) 455-459. https://doi.org/10.1016/0038-1101(90)90050-O

[2] H.-Y. Chou, E. O'Connor, A. O'Mahony, I. M. Povey, P. K. Hurley, Lin Dong, P. D. Ye, V. V. Afanas'ev, M. Houssa, A. Stesmans, Band offsets and trap-related electron transitions at interfaces of (100)InAs with atomic-layer deposited Al_2O_3, J. Appl. Phys. 120 (2016) 235701 (1-7). https://doi.org/10.1063/1.4971178

[3] V. V. Afanas'ev, A. Stesmans, Internal photoemission at interfaces of high-k insulators with semiconductors and metals, J. Appl. Phys. 102 (2007) 081301 (1-28). https://doi.org/10.1063/1.2799091

[4] I. Shlyakhov, J. Chai, M. Yang, S. J. Wang, V. V. Afanas'ev, M. Houssa, A. Stesmans, Band alignment at interfaces of synthetic few-monolayer MoS_2 with SiO_2 from internal photoemission, APL Materials 6 (2018) 026801(1-5). https://doi.org/10.1063/1.5002617

[5] D. Chiappe, J. Ludwig, A. Leonhardt, S. El Kazzi, A. N. Mehta, T. Nuytten, U. Celano, S. Sutar, G. Pourtois, M. Caymax, K. Paredis, W. Vandervorst, D. Lin, S. De Gendt, K. Barla, C. Huyghebaert, I. Asselberghs, I. Radu, Layer-controlled epitaxy of 2D semiconductors: bridging nanoscale phenomena to wafer-scale uniformity, Nanotechnology 29(2018) 425602 (1-9). https://doi.org/10.1088/1361-6528/aad798

[6] V. Afanas'ev, D. Chiappe, C. Huyghebaert, I. Radu, S. De Gendt, M. Houssa, A. Stesmans, Band alignment at interfaces of few-monolayer MoS_2 with SiO_2 and HfO_2, Microel. Eng.147 (2015) 294 297. https://doi.org/10.1016/j.mee.2015.04.106

[7] Z. Zhang, C. M. Jackson, A. R. Arenhart, B. McSkimming, J. S. Speck, S. A. Ringel, Direct Determination of Energy Band Alignments of $Ni/Al_2O_3/GaN$ MOS Structures Using Internal Photoemission Spectroscopy, J. Electron. Mater.43 (2014) 828-832. https://doi.org/10.1007/s11664-013-2942-z

[8] P. M. Solomon, D. J. DiMaria, Effect of forming gas anneal on Al-SiO_2 internal photoemission characteristics, J. Appl. Phys. 52 (1981) 5867-5869. https://doi.org/10.1063/1.329460

[9] B. Groven, A. N. Mehta, H. Bender, J. Meersschaut, Th. Nuytten, P. Verdonck, T. Conard, Q. Smets, T. Schram, B. Schoenaers, A. Stesmans, V. Afanas'ev, W. Vandervorst, M. Heyns, M. Caymax, I. Radu, A. Delabie, Two-Dimensional Crystal Grain Size Tuning in WS_2 Atomic Layer Deposition: An Insight in the Nucleation Mechanism, Chem. Mater. 30 (2018) 7648-7663. https://doi.org/10.1021/acs.chemmater.8b02924